MOLECULAR PHYSICS REPORTS **38** (2003) 47-55

ELECTRONIC STRUCTURE AND THERMODYNAMICAL PROPERTIES OF SOME TERNARY *d* AND *f* ELECTRON INTERMETALLICS

ANDRZEJ ŚLEBARSKI[1] and ANDRZEJ JEZIERSKI[2]

[1]*Institute of Physics, University of Silesia, 40-007 Katowice, Poland*

[2]*Institute of Molecular Physics, Polish Academy of Sciences 60-179 Poznań, Poland*

Abstract: We have discussed structural and magnetic properties and electronic structure of the ternary CeMSn and CeMSb compounds, where M is a transition metal. The main goal of this presentation is to find the influence of the electronic properties of the metal M on the coherent gap formation in the ternary Ce-Kondo insulators.

1. ELECTRONIC STRUCTURE OF CeNiSn AND CeRhSb

Recently we have been interested in the Ce-based intermetallics with a coherent ground state (the gap) in the Kondo lattice. The compounds CeNiSn and CeRhSb are only two in the equiatomic ternary series which show this hybridization gap in the electronic density of states (DOS) at low temperatures and a paramagnetic ground state [1, 2]. The class of these materials, i.e., "Kondo insulators" [3] is characterized by their electronic properties, which at high temperatures are associated with a set of independent localized 4*f* moments interacting with the conduction electrons (CE), while at low temperatures the electronic properties resemble those of narrow gap of the order ~10 K. In terms of a simple Kondo model, the gap would also correspond to the filling of the Brillouin zone by additional states due to the Abrikosov-Suhl resonance [4]. In this picture, the hybridization involves one occupied *f*-state crossing exactly one half-filled conduction band, crossing more than one band leads to a metallic state. At $T < T_K$, where T_K is a Kondo temperature, the Kondo resonance forms a filled Brillouin zone and a gap of size order $k_B T_K$ separates the filled and empty states. In this model the temperature-dependent properties of these insulators seem more easily described at $T > T_K$ as the thermally induced appearance of localized *f* electrons, each thermal excitation yields one conduction electron. An insulating gap formation is indeed theoretically expected for Kondo systems without long-range magnetic order and with a certain Coulomb interaction between *f* states ($U \neq 0$) [5]. Materials where the electron interaction energies dominate the electron kinetic energies are well known as strongly correlated electron systems. In band-structure calculations, the Ce 4*f* electrons are treated as band electrons. In reality, they are more localized, and to treat them correctly, band theory would have to include also local correlations. These correlations could cause the numerical changes in the DOS, however, the numerical calculations are very difficult. One way to explore this issue would be to carry out the calculations treating the Ce 4*f* as a frozen core states, which do not hybridize with CE. The numerical results for CeRhSb with the Ce 4*f* electrons as band electrons and with 4*f* states as a frozen core states are presented in Fig. 1. The calculations for the frozen 4*f* core state have never given the gap and the DOS at the Fermi level is much higher than for the 4*f* electrons treated as band electrons [6]. Therefore, the charge fluctuations (valence

instabilities) of Ce ions are very important to understand the physics of these systems, e.g., they can reduce the magnetic correlations in these compounds [7].

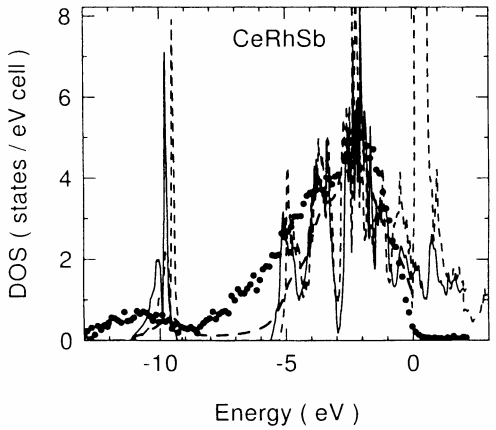

Fig. 1. CeRhSb; comparison of the XPS valence band spectra corrected by the background and the numerical results with the Ce 4*f* electrons treated as band electrons (dotted line) and with the Ce 4*f* as a frozen core state (solid line). For comparison we also present the convoluted DOS (*f* electrons are itinerant) by Lorentzians of the half-width 0.4 eV and taking into account proper cross sections for bands with different *l* symmetry; heavy dashed line

In conclusion, band-structure calculations on Ce-based "Kondo insulators" show that a *V*-shaped pseudogap formation is strongly dependent on the *f*-conduction electron hybridization. Replacing all of the Ce ions in a Kondo insulator with trivalent ions leads to an ordinary metallic state (e.g., in [8]), whereas by replacing the Ce ions with tetravalent non-*f*-electron ions, such as Zr, Ti, or Hf ions, a semiconducting state is obtained. Accordingly, the gap ~400 meV in ZrNiSn is destroyed if Ni is replaced by another transition element [9]. This gap can also be suppressed by a partial substitution of a trivalent metal (e.g., Ce) for Zr^4+, despite the fact that electronic structures of the ZrNiSn and CeNiSn are rather simple and similar [9, 10]. In Figure 2a the calculated bands are shown for CeNiSn, when Ce is substituted by trivalent La. We note indirect gaps near the Fermi level that are strongly suppressed with alloying. Figure 2b shows the Ce 3*d* XPS spectra, which exhibit a rapid decrease of the $3df^0$ peak intensity for $Ce_{1-x}La_xNiSn$ alloys, when x is larger than 0.05 [11].

The ground states of CeNiSn and CeRhSb are nonmagnetic, and in both cases Ce have unstable *f*-configuration. The X-ray Photoemission Spectroscopy (XPS) spectra of the 3*d* and 4*d* core levels give information about the 4*f* shell configurations and *f*-conduction electron hybridization. The intensity of the 3*d* lines in the Ce intermetallic compounds shows different final states depending on the occupation of the *f* shell [12, 13]. Figure 3 represents the Ce 3*d* XPS spectra of CeNiSn (a), CeRhSb and CePdSb (b), respectively. Three final-state contributions f^1, and f^2 are clearly observed, which exhibit a spin-orbit splitting $\Delta_{SO} \cong 18.4$ eV. The appearance of the $3d^9f^0$ component in the 3*d* XPS spectrum of CeNiSn [10] and CeRhSb [9] is clear evidence of the intermediate valence behavior of Ce. Based on the Gunnarsson-Schönhammer theoretical model [12, 13], the intensity ratio $I(f^0)/(I(f^0) + I(f^1) + I(f^2))$, which should be directly related to the *f*-occupation probability in the final states, indicates an *f*-occupation number n_f^{XPS}. The separation of the overlaping peaks in the Ce 3*d* XPS spectra was made on the basis of the Doniach-Šunjić theory [14]. The occupation number of the *f* shell n_f^{XPS} experimentally obtained from the Ce 3*d* XPS spectra is respectively 0.93 (CeRhSn), and 0.95

a

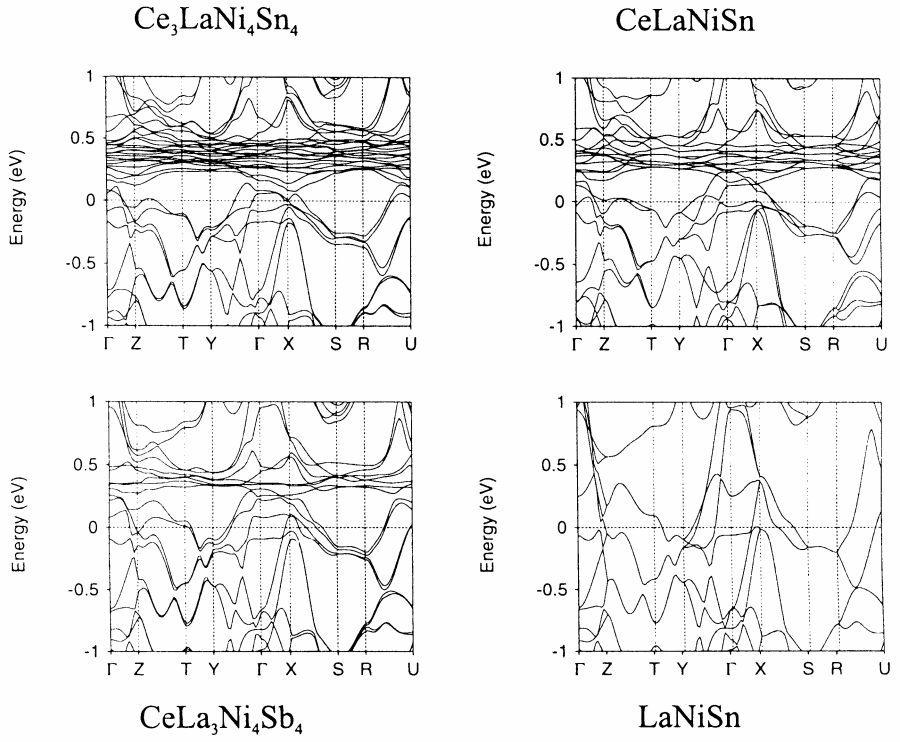

b

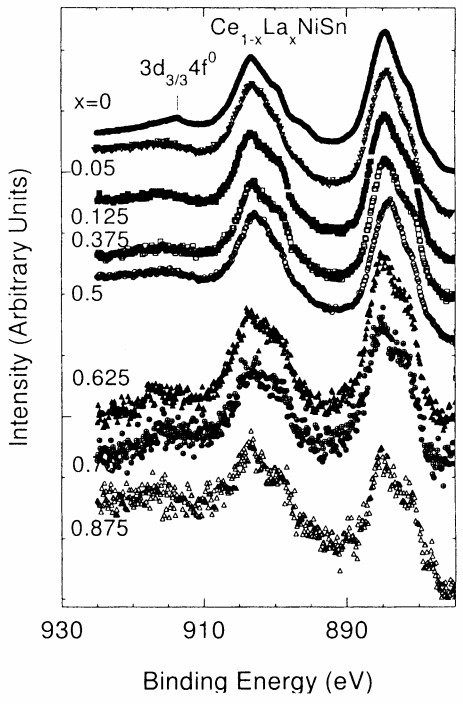

Fig. 2. (a) TB LMTO band structure of $Ce_{1-x}La_xNiSn$ along various symmetry directions in the Brillouin zone; $x = 0.25, 0.5, 0.75$, and 1 (b) Ce $3d$ XPS spectra obtained for several $Ce_{1-x}La_xNiSn$ alloys. Δ_{SO} is a spin-orbit-split energy. The spectra consist of $3d_{3/2}$ and $3d_{5/2}$ components with additional peaks at higher ($3d^9f^0$) and lower ($3d^9f^2$) energies, respectively [11]

(CeNiSn). The $3d^9f^2$ components in the Ce $3d$ XPS spectra in Fig. 3 are attributed within the Gunnarsson-Schönhammer model to f-conduction electron hybridization. The hybridization energy Δ, which describes the hybridization part of the Anderson impurity Hamiltonian [15], is defined as $\pi V_{sf}^2 \rho_{max}$, where ρ_{max} is the maximum in the DOS and V_{sf} is the hybridization matrix element. It is possible to estimate Δ from the ratio $r = I(f^2)/(I(f^1) + I(f^2))$, calculated as a function of Δ in Ref. [13], when the peaks of the Ce $3d$ XPS spectra that overlap in Fig. 3 are separated [14]. Figure 3b compares the Ce $3d$ XPS spectra obtained for CeRhSb and CePdSb, which indicates stronger hybridization between $4f$ and CE and mixed valence character of Ce in CeRhSb. The intensity ratio gives for CeNiSn and CeRhSb a crude estimate of a hybridization width ~150 meV, while for CePdSb Δ is only ~50 meV [16]. The changed number of electrons in the valence band due to alloying can destroy the charge gap. CePdSb [17] and CeNiSb [18] are good examples, where alloying provides an extra electron to the conduction band, which can change the DOS in the vicinity of the gap and move the Fermi level.

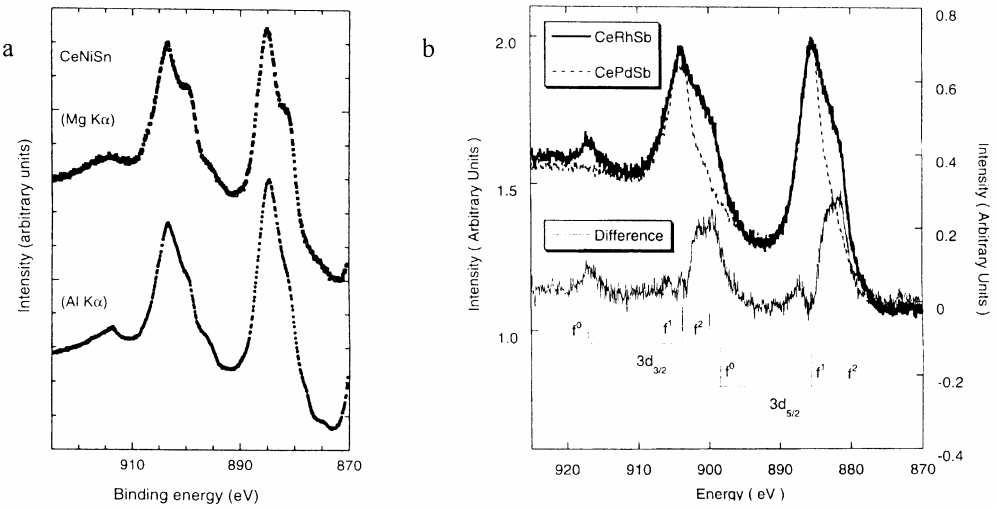

Fig. 3. (a) The Ce $3d$ XPS spectra obtained for CeNiSn with Mg K_α and Al K_α. (b) Ce $3d$ XPS spectra obtained for CeRhSb and CePdSb and the difference of the intensities [16]

In Figure 4a we compare the photoemission spectra for $h\nu = 21.2$ (HeI), 40.8 (HeII) and 1486.6 eV (Al K_α) with the LMTO calculations for CeNiSn. The spectra demonstrate a valence band that has a major peak that is mainly due to the d states located near the Fermi level. The second peak centered at about 8 eV is due to the Sn s states, it is observed for CeRhSn (Fig. 4b), while for CeNiSn the 8 eV peak is only just detectable. All the photoemission spectra are subtracted from the background which has been calculated using the well established Tougaard algorithms [19]. The partial DOSs in both cases show a renormalized f level and the calculated ground states are non-magnetic. In band-structure calculations, the Ce $4f$ electrons are treated as itinerant, they are distributed near the Fermi level (ϵ_f). The $4f$ states hybridize in the band with the CE and the transition-metal d states. This hybridization can lead to the formation of a gap, for example in the DOS of CeRhSb or CeNiSn, while the DOS presented in Fig. 4b only signals a tendency to gap formation in the bands of CeRhSn. An indirect gap

having a very small number of the electronic states at ϵ_{F}, results from LMTO calculations in the partial DOSs of Rh and Sn, while Ce gives a main contribution to the total DOS at ϵ_{F}.

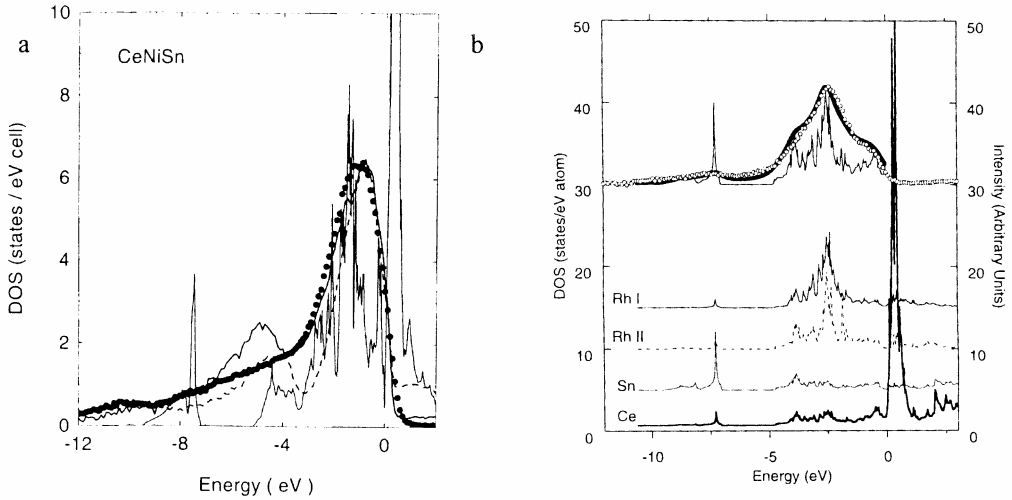

Fig. 4. (a), CeNiSn; the DOS are compared with the valence band XPS spectra (points) and with the measured $h\nu = 21.2$ (line) and 40.8 eV (dotted line) UP spectra. (b) Comparison of the total DOS calculated for paramagnetic CeRhSn (light curve), convoluted by Lorentzians of half-width 0.4 eV, taking into account proper cross sections for bands with different l symmetry (heavy curve), and measured XPS valence bands corrected by the background (open points). The partial DOS curves for Ce, Rh_I at (0 0 1/2), Rh_{II} at (1/3 2/3 0) and Sn are plotted below [20]

In Ref. [20] we have tried to explain the contributions which remove a gap in CeRhSn, considering the fractional valence of Ce ions, which is compared with that of the well-known Kondo insulators, e.g., CeNiSn or CeRhSb and its hybridization energy Δ between the *f*- and CE states. The volume of the unit cell of CeRhSn, which is much larger than that of CeNiSn or CeRhSb, could be a reason; in result the conduction band narrows, the DOS of the *f* states is enhanced at ϵ_{F}, and the *f*-electrons are more localized and leads to the local correlations in CeRhSn.

2. VOLUME EFFECT

We will discuss the properties of the compositionally similar compounds CeMSn to CeNiSn, and CeMSb to CeRhSb, when Ni or Rh is replaced by neighbour transition metal M in the periodic table. Only CeNiSn and CeRhSb have a hybridization gap, while the remaining compounds are magnetic and nonsemiconducting materials. The key ingredient of the mechanism of the magnetic ground state is the competition between the Kondo energy (T_K) and the RKKY coupling between the local moments. While the RKKY interaction temperature $T_{RKKY} \propto J_{sf}^2 \rho(\epsilon_F)$, where $\rho(\epsilon_F)$ is DOS at the Fermi level, the Kondo temperature is given by $T_K \propto \exp(-1/|J_{sf}\rho(\epsilon_F)|)$, where $J_{sf} \propto -|V_{sf}|^2/E_{4f}$ in the limit of infinite interatomic Coulomb repulsion [22]. Since in general the hybridization matrix element (and hence the Kondo coupling)

between the conduction and Ce *f*-electrons decreases with increasing volume of the unit cell of CeMSn with respect to CeNiSn, the RKKY interaction dominates over the Kondo effect and magnetic ordering can occur as in the case of CePdSn [21], CeCuSn [23], or CeAgSn [24]. An analogous situation is in the CeMSb series of alloys.

The ground state of CeRhSn is very unusual; heavy fermion behavior is observed in the presence of magnetic clusters. The structure of CeRhSn contains planes in which the distance between Ce ions, $d_{\text{Ce-Ce}}$ = 3.89 Å, is very large and very close to the Hill limit [25], whereas perpendicular to these planes, the spacing between Ce ions is much larger. Consequently, the direct *f-f* overlap is negligible, and the hybridization, mainly between Ce 4*f* and Rh 4*d* states could lead to magnetic interaction between Ce ions. The experiments described below suggest that atomic disorder plays an important role in the anomalous behavior observed in the low-temperature physical properties of CeRhSn.

In conclussion, a volume effect modifies the conduction electron band-width either in CeNiSn or CeRhSb if Ni or Rh is replaced by another transition metal M. The doping at Ni or Rh sites leads to an increase in the unit cell volume, which reduces the Kondo coupling J_{sf}, and the system usualy has a magnetic ground state.

2.1. CeNiSb and CePdSb

CeNiSb [26, 18] and CePdSb [27, 16] are examples of the few ternary compounds which exhibit Kondo lattice behavior in their electrical transport properties together with a ferromagnetic ground state. CeNiSb as well as CePdSb show competition between magnetic and Kondo interactions consistent with expectations based on the Doniach phase diagram [28]. The quantity $|J_{sf}\rho(\epsilon_F)|$ increases smoothly with pressure P in Ce alloys and compounds [29, 30]. Doniach considered the competition between RKKY and Kondo interaction theoretically in a one-dimensional Kondo lattice [28]. His phase diagram has been shown to give a good qualitative description of the resistivity ρ *vs* P results for many Ce-based compounds that display a well-defined maximum in $T_C(P)$.

Recently we have shown [16] that the magnetic behavior of the Kondo lattice compounds CeNiSb and CePdSb can be explained in terms of the Doniach phase diagram. The hybridization energy Δ obtained from the 3*d* XPS spectra allowed us to estimate $|J_{sf}\rho(\epsilon_F)|$, which is ~0.15 for CeNiSb and ~0.6 for CePdSb. We therefore located both compounds on the left side of the maximum in the T_C - $|J_{sf}\rho(\epsilon_F)|$ phase diagram, however, CeNiSb lies at the beginning in the plot of T_C *vs* P, while CePdSb is nearer the maximum. In terms of the Doniach diagram CePdSb displays a maximum in $T_C(P)$ [31] predicted by Doniach phase diagram, while for CeNiSb T_C is linear *vs* P at various applied hydrostatic pressures up to 18.6 kbar [18]. Since the unit cell volume of CeNiSb is smaller than that of CeRhSb, a large volume of the Kondo coupling constant J_{sf} was used to explain the lower T_C in CeNiSn (~4 K) in Ref. [26] due to the smaller distance between the Ce ions (the Curie temperature for CePdSb is ~17 K).

2.2. CeRhSn

The competition between the Kondo and RKKY interaction can induce a zero-temperature magnetic-nonmagnetic transition, which leads to deviations from the standard Fermi liquid (FL) scaling of bulk physical properties. For a Landau FL at a very small temperatures, the specific

heat C divided by temperature T, C/T, and the magnetic susceptibility χ approach constant values, while the electrical resistivity $\rho \propto T^2$.

An increasing number of Ce-based heavy fermion metals were shown to display pronounced deviations from the properties of LFL. In particular, $\rho \sim T^{\varepsilon}$ with exponents $1 \leq \varepsilon < 2$, C/T and χ diverges logarithmically with decreasing T or shows T^{-n} dependence with $n < 1$, when the Ce-based HF compounds are tuned through an antiferromagnetic quantum critical point (QCP) by varying a control parameter such as chemical composition, pressure, or magnetic field [32-34]. The QCP can be thought to result from the competition between the Kondo screening of the magnetic moments and the antiferromagnetic correlations due to RKKY interaction [28, 35].

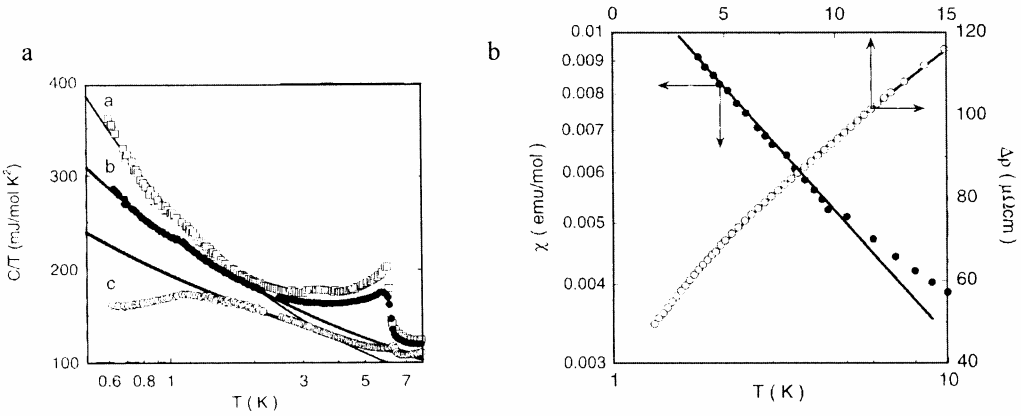

Fig. 5. (a), Specific heat C divided by T, C/T, *versus* ln$T$ for three CeRhSn samples (sample (a) -non-annealed; samples (b) and (c) -annealed for 4 and 8 days, respectively) [20]. The C/T data were fitted by the formula $C(T)/T = cT^{-n}$ in the range $T < 2$ K for samples (a) and (b), and in the range $1.5 < T < 5$ K for sample (c). The fits are represented by solid lines. The values of c are, respectively: 246.4 mJmol^{-1}K^{-3}, 235.9 mJmol^{-1}K^{-3}, and 195.8 mJmol^{-1}K^{-3} for samples (a), (b), and (c) and n values are: 0.46, 0.61, and 0.65. (b), Magnetic susceptibility χ versus T on a double logarithmic plot and the incremental electrical resistivity $\Delta\rho = \rho$(CeRhSn) - ρ(LaRhSn) *versus* T for a CeRhSn sample annealed for 8 days (sample (c)). The solid line represents the fit of the expression $\Delta\rho(T) = \Delta\rho(0)[1 + a(T/T_K)^n]$ to the data with $n = 0.74$, $\Delta\rho(0) = 32.2$ μΩcm, $a = 13.9$ and $T_K = 145$ K. The straight line represents the relation $\chi \propto T^{-n}$, where $n = 0.49$

Non-Fermi liquid behavior is often observed to occur in the presence of atomic disorder [36, 37]. Very recently we have observed NFL behavior in CeRhSn, which may be related to atomic disorder [20]. At the lowest temperatures the electrical resistivity $\Delta\rho = \rho - \rho_0 \propto T^{\varepsilon}$ ($\varepsilon = 0.93$), and $\chi(T) \propto C(T)/T \propto T^{-n}$ ($n \cong 0.5$).

The specific heat data for non-annealed CeRhSn (sample (a)) and for CeRhSn samples annealed for 4 days (sample (b)) and 8 days (sample (c)) are displayed as C/T *versus* ln T in Fig. 5. The high temperature specific heat data are very similar for all the samples investigated [20] while, at temperatures lower then about 6.2 K, the magnetic contribution to the specific heat is strongly dependent on the amount of atomic disorder. The atomic-sphere approximation by the self-consistent TB LMTO method and the local-spin-density approximation yields a magnetic moment per formula unit for a disordered Ce-Rh-Sn alloys, while the ground state of the CeRhSn compound calculated with atomic order produces a nonmagnetic result. Assuming that

the crystalline electric field ground state is a doublet, the total magnetic entropy per formula unit of CeRhSn is $R\ln 2 = 5.76\ \mathrm{J\,mol^{-1}K^{-2}}$. The small peak in the specific heat of CeRhSn observed at T_N represents an extremally small fraction $\gamma T_N/R\ln 2$ which is respectively ~0.12, 0.06, and 0.02 of entropy $R\ln 2$ at the phase transition for samples (a), (b), and (c). We have not seen any magnetic order within a limit of about 0.25 μ_B, using a high-resolution neutron spectrometer [20]. Some type of static magnetic order in CeRhSn with tiny ordered moments less than 0.1 μ_B is probably due to subtle structural defects [38].

Figure 5 reveals that C/T varies as T^{-n} below 2 K for sample (a) and (b), while it varies as T^{-n} between 1.5 K and 5 K for CeRhSn annealed for 8 days (sample (c)). The best fit of the expression $C(T)/T = cT^{-n}$ to the data yields $n = 0.54$ for sample (a), $n = 0.39$ for sample (b) and $n = 0.35$ for sample (c). The parameters obtained from the best fits are consistent with the presence of a Griffiths phase at very low temperatures; i.e., $C/T \propto \chi \propto T^{-1+\lambda}$, with $\lambda < 1$.

3. CONCLUDING REMARKS

CeMSn and CeMSb ternary alloys with transition metal M have a number of different ground states including magnetic (e.g., CePdSb) and nonmagnertic (e.g., CeNiSn, CeRhSb), metallic and insulating. They exhibit anomalous physical properties such as: Heavy Fermion, Fermi liquid and non-Fermi liquid behavior, e.c.t. CeNiSn and CeRhSb are only two in equiatomic ternary series that show a hybridization gap in electronic density of states at Fermi level, while the others are antiferromagnetic (e.g., CeCuSn, CeAgSn, CePdSn) or ferromagnetic (e.g., the equiatomic antimonides CeMSb, M: Ni, Pd, Pt). The hybridization gap formed at the Fermi level is strongly reduced by doping due to formation of the Kondo holes band.

Acknowledgments

AŚ would like to thank the Polish State Committee for Scientific Research (KBN) for financial support from Project No 2 P03B 098 25. The work was supported by the Centre of Excellence for Magnetic and Molecular Materials for Future Electronics within the European Commission contract No. G5MA-CT-2002-04049.

References

[1] T. Takabatake, F. Teshima, H. Fujii, S. Nishigori, T. Suzuki, T. Fujita, Y. Yamaguchi, J. Sakurai, D. Jaccard, Phys. Rev. **B41**, 9607 (1990).
[2] M. F. Hundley, P. C. Confield, J. D. Thompson, Z. Fisk, Phys. Rev. **B42**, 6842 (1990).
[3] It has been controversial whether or not the ground state of CeNiSn or CeRhSb is in a semiconducting or in a semimetallic state with very low carrier density of states with a *V*-shape pseudogap. NMR experiments (K. I. Nakamura et al., Phys. Rev. **B54**, 6062 (1996)) showed that the Fermi level is in the *V*-shape gapped structure of CeNiSn, which was classified as a semimetal with a low DOS. The problem of the ground state of CeNiSn and CeRhSb is still under discussion.
[4] Z. Fisk, J. L. Sarrao, J. D. Thompson, D. Mandrus, M. F. Hundley, A. Miglori, B. Bucher, Z.Schlesinger, G. Aeppli, E. Bucher, J. F. DiTusa, C. S. Oglesby, H-R. Ott, P. C. Confield, S. E. Brown, Physica B **206-207**, 798 (1995).
[5] R. M. Martin, Phys. Rev. Lett. **48**, 362 (1982).
[6] A. Ślebarski, A. Jezierski, A. Zygmunt, S. Mähl, M. Neumann, Phys. Rev. **B58**, 13498 (1998).
[7] C. M. Varma, Phys. Rev. **B50**, 9952 (1994).

[8] A. Szytula and J. Leciejewicz, *Handbook of the Physics and Chemistry of Rare Earths*, eds. K. A. Gschneidner Jr, L. Eyring, North-Holland, Amsterdam 1989, chap. 83, p.133.
[9] A. Ślebarski, A. Jezierski, A. Zygmunt, S. Mähl, M. Neumann, Phys. Rev. **B57**, 9544 (1998).
[10] A. Ślebarski, A. Jezierski, A. Zygmunt, S. Mähl, M. Neumann,G. Borstel, Phys. Rev. **B54**, 13551 (1996).
[11] A. Ślebarski, A. Jezierski, S. Mähl, M. Neumann, G. Borstel, Phys. Rev. **B58**, 4367 (1998).
[12] O. Gunnarsson and K. Schönhammer, Phys. Rev. **B28**, 4315 (1983).
[13] J. C. Fuggle, F. U. Hillebrecht, Z. Zolnierek, R. Lässer, Ch. Freiburg, O. Gunnarsson, K. Schönhammer, Phys. Rev. **B27**, 7330 (1983).
[14] S. Doniach and M. Šunjić, J. Phys. **C3**, 286 (1970).
[15] P. W. Anderson, Phys. Rev. **124**, 41 (1961).
[16] A. Ślebarski, M. Radlowska, A. Zygmunt, A. Jezierski, Phys. Rev. **B65**, 205110 (2002).
[17] Latika Menon and S. K. Malik, Phys. Rev. **B55**, 14100 (1997).
[18] A. Ślebarski, E. D. Bauer, Shi Li, M. B. Maple, A. Jezierski, Phys. Rev. **B63**, 125126 (2001).
[19] S. Tougaard and P. Sigmund, Phys. Rev. **B25**, 4452 (1982).
[20] A. Ślebarski, M. B. Maple, E. J. Freeman, C. Sirvent, M. Radlowska, A. Jezierski, E. Granado, Qing-zhen Huang, J. W. Lynn, Phil. Mag. **B82**, 943 (2002).
[21] S. K. Malik, D. T. Adroja, S. K. Dhar, R. Vijayaraghavan, B. D. Padalia, Phy. Rev. **B40**, 2414 (1989).
[22] J. R. Schrieffer and P. A. Wolff, Phys. Rev. **149**, 491 (1966).
[23] J. Sakurai, K. Kegai, K. Nishimura, Y. Ishikawa, K. Mori, Physica **B186-188**, 583 (1993).
[24] J. Sakurai, S. Nakatani, A. Adam, H. Fujiwara, J. Magn. Magn. Mater. **108**, 143 (1992).
[25] H. H. Hill, in: *Plutonium 1970 and Other Actinides*, ed. W. N. Miner (AIME), 1970, pp. 1-19.
[26] Latika Menon and S. K. Malik, Phys. Rev. **B52**, 35 (1995).
[27] S. K. Malik and D. T. Adroja, Phys. Rev. **B43**, 6295 (1991).
[28] S. Doniach, in: *Valence Instability and Related Narrow Band Phenomena*, ed. R. D. Parks (Plenum, New York, 1977).
[29] M. B. Maple and D. Wohlleben, *Magnetism and Magnetic Materials-1973*, ed. C. P. Graham, Jr. and J. J. Rhyne, AIP Conf. Proc. No. 18 (AIP, New York, 1973), p. 447.
[30] J. S. Schilling, Adv. Phys. **28**, 657 (1979).
[31] A. L. Cornelius, A. K. Gangopadhyay, J. S. Schilling, W. Assmus, Phys. Rev. **B55**, 14109 (1997).
[32] H. V. Löhneysen, J. Phys.: Condens. Matter **8**, 9689 (1996).
[33] N. D. Mathur, Nature (London) **394**, 39 (1998).
[34] K. Heuser, E.-W. Scheidt, T. Schreiner, G. R. Stewart, Phys. Rev. **B57**, R4198 (1998).
[35] S. Doniach, Physica **B91**, 231 (1977).
[36] O. O. Bernal, D. E. MacLaughlin, H. G. Lukefahr, B. Andraka, Phys. Rev. Lett. **75**, 2023 (1995).
[37] A. H. Castro Neto, G. Castilla, B. A. Jones, Phys. Rev. Lett. **81**, 3531 (1998).
[38] A. Ślebarski, M. Radrowska, T. Zawada, M. B. Maple, A. Jezierski, A. Zygmunt, Phys. Rev. **B66**, 104434 (2002).